AGU PUBLICATIONS

Geophysical Research Letters

RESEARCH LETTER
10.1002/2016GL069049

Key Points:
- We developed a methane model that represents high-affinity methanotrophy and active microbial biomass changes in arctic mineral soils
- High-affinity methanotrophy facilitated accurate simulation of methane consumption in arctic mineral soils
- Active microbial biomass changes strongly influenced seasonal methane fluxes

Supporting Information:
- Supporting Information S1

Correspondence to:
D. Medvigy,
dmedvigy@princeton.edu

Citation:
Oh, Y., et al. (2016), A scalable model for methane consumption in arctic mineral soils, *Geophys. Res. Lett.*, *43*, 5143–5150, doi:10.1002/2016GL069049.

Received 8 APR 2016
Accepted 17 MAY 2016
Accepted article online 19 MAY 2016
Published online 31 MAY 2016

A scalable model for methane consumption in arctic mineral soils

Youmi Oh[1], Brandon Stackhouse[2], Maggie C. Y. Lau[2], Xiangtao Xu[2], Anna T. Trugman[1], Jonathan Moch[2,3], Tullis C. Onstott[2], Christian J. Jørgensen[4], Ludovica D'Imperio[4], Bo Elberling[4], Craig A. Emmerton[5], Vincent L. St. Louis[5], and David Medvigy[1,2]

[1]Program in Atmospheric and Oceanic Sciences, Princeton University, Princeton, New Jersey, USA, [2]Department of Geosciences, Princeton University, Princeton, New Jersey, USA, [3]Now at Department of Earth and Planetary Sciences, Harvard University, Cambridge, Massachusetts, USA, [4]Center for Permafrost (CENPERM), Department of Geosciences and Natural Resource Management, University of Copenhagen, Copenhagen, Denmark, [5]Department of Biological Sciences, University of Alberta, Edmonton, Alberta, Canada

Abstract Recent field studies have documented a surprisingly strong and consistent methane sink in arctic mineral soils, thought to be due to high-affinity methanotrophy. However, the distinctive physiology of these methanotrophs is poorly represented in mechanistic methane models. We developed a new model, constrained by microcosm experiments, to simulate the activity of high-affinity methanotrophs. The model was tested against soil core-thawing experiments and field-based measurements of methane fluxes and was compared to conventional mechanistic methane models. Our simulations show that high-affinity methanotrophy can be an important component of the net methane flux from arctic mineral soils. Simulations without this process overestimate methane emissions. Furthermore, simulations of methane flux seasonality are improved by dynamic simulation of active microbial biomass. Because a large fraction of the Arctic is characterized by mineral soils, high-affinity methanotrophy will likely have a strong effect on its net methane flux.

1. Introduction

Arctic soils constitute an important methane source to the atmosphere. Mechanistic methane models and observation-based atmospheric inversions indicate a net arctic methane source in the range +15–30 Tg CH_4 yr^{-1} [*Tan et al.*, 2015]. Furthermore, mechanistic methane models indicate that methane emissions from the Arctic may increase with temperatures and permafrost thaw [*McGuire et al.*, 2009; *Schaefer et al.*, 2011; *Koven et al.*, 2013; *Schuur et al.*, 2013].

However, not all arctic locations are methane sources. Recent field studies have identified multiple sites that are net methane sinks [*Zhu et al.*, 2012; *Brummell et al.*, 2014; *Emmerton et al.*, 2014; *Martineau et al.*, 2014; *Jørgensen et al.*, 2015; *Lau et al.*, 2015; *Stackhouse et al.*, 2015]. The cryosols associated with methane sinks are drier, more oxic, and contain less soil organic carbon (SOC) than methane-emitting, SOC-rich wetlands. SOC-poor cryosols span 87% of the Arctic [*Hugelius et al.*, 2014]. Because mechanistic methane models have been parameterized using observations of SOC-rich soils and anaerobic conditions [*Melton et al.*, 2013; *Wania et al.*, 2013; *Zhuang et al.*, 2013], it is not obvious that they can accurately simulate the net methane uptake associated with dry cryosols or predict how methane fluxes associated with such cryosols will evolve with further warming.

The net methane flux in arctic soils can potentially be explained by biogeographic differences in methanotroph community composition [*Christiansen et al.*, 2015]. In wet, SOC-rich soils, methane production by methanogenic archaea (hereafter, methanogens) is typically larger than methane oxidation by methanotrophic bacteria (hereafter, methanotrophs), with the surplus methane released into the atmosphere [*Le Mer and Roger*, 2001]. The dominant methanotrophs in SOC-rich soils are classified as "low affinity" and require methane concentrations in excess of 600 ppmv for growth and maintenance [*Conrad*, 2009]. But in drier mineral arctic cryosols, the dominant ("high-affinity") methanotrophs can survive at atmospheric methane concentrations [*Lau et al.*, 2015]. Soil incubation experiments have shown that high-affinity methanotrophs are about 2–3 times as sensitive to temperature as low-affinity methanotrophs [*Christiansen et al.*, 2015; *Jørgensen et al.*, 2015; *Lau et al.*, 2015] and that high-affinity methanotrophs have surprisingly high activity under saturated soil moisture conditions

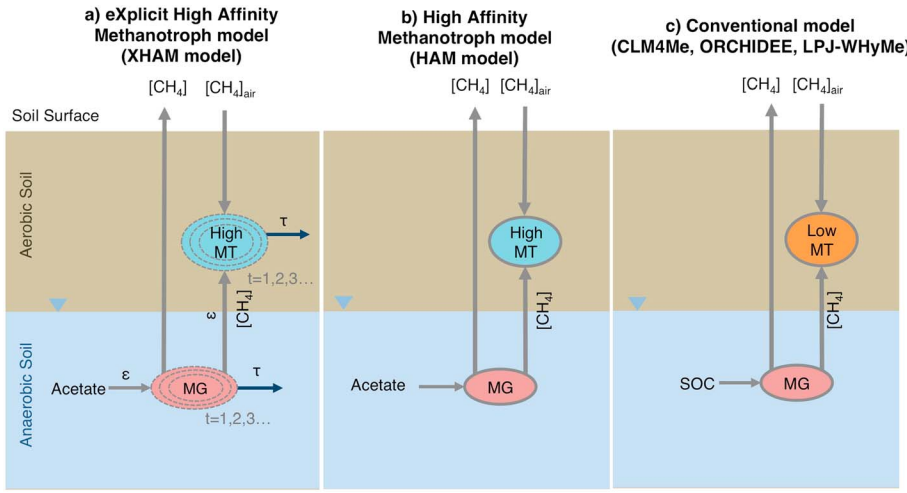

Figure 1. Main configuration of three classes of methane models. Models simulate methane production by methanogens (MG), methane oxidation by methanotrophs (MT), and vertical methane transport by diffusion. Methanogens occupy soils with high volumetric water content, whereas methanotrophs occupy moderate volumetric water content. (a) Our eXplicit High-Affinity Methanotroph model (XHAM) considers acetate as a substrate for methane production. High-affinity methanotrophs (high MT) consume methane ($[CH_4]$) produced by methanogens and atmospheric methane ($[CH_4]_{air}$). XHAM also computes active biomass changes of acetoclastic methanogens and high-affinity methanotrophs using carbon use efficiencies (ε) and microbial turnover rates (τ). (b) Our High-Affinity Methanotroph model (HAM) has a structure similar to XHAM except that the active microbial biomass is fixed. (c) Conventional models simulate methane production via decomposition of soil organic carbon (SOC), and the majority of methane is transported above ground. Low-affinity methanotrophs (low MT) consume some of the methane produced by methanogens.

[*Stackhouse et al.*, 2015]. These characteristics may allow high-affinity methanotrophs to oxidize more methane as temperatures increase. Some recent mechanistic models have included parameterizations of high-affinity methanotrophs, but model parameters have not been constrained by observations from arctic mineral soils [*Riley et al.*, 2011; *Ringeval et al.*, 2010].

Changes in active biomass may explain why seasonal variations in methane fluxes lag behind seasonal variations in air temperature [*King*, 1994] and have been shown to be important for understanding methanotrophy [*Shukla et al.*, 2013]. But growth rates in natural arctic settings are generally slow, and it is unknown whether high-affinity methanotrophs can grow at atmospheric methane concentrations. Thus, we chose to model the changes in active biomass that would come about during thaw by the repair of critical enzymes in microorganisms that had been dormant during the winter rather than a net increase in total cellular abundance. A recent methane model has included microbial dynamics [*Xu et al.*, 2015]; however, the model dynamics were not tested at field scales.

We test two hypotheses: (1) the representation of high-affinity methanotrophs facilitates accurate simulation of atmospheric methane consumption in arctic mineral cryosols; and (2) explicit consideration of the active methanotroph biomass improves simulated seasonal methane fluxes. To evaluate these hypotheses, we present a new model and evaluate it against laboratory and field measurements of methane fluxes.

2. Materials and Methods

2.1. Model Description

We developed a methane model (eXplicit High-Affinity Methanotroph model; "XHAM") that includes both high-affinity methantrophs and active microbial biomass dynamics (Figure 1a). To isolate the effect of active microbial biomass changes, we compared simulations from XHAM to simulations from a simplified model that did not include active microbial biomass dynamics (High-Affinity Methanotroph model; "HAM") (Figure 1b). We compared our XHAM and HAM results to simulations from three established mechanistic methane models (CLM4Me, ORCHIDEE, and LPJ-WHyMe) (Figure 1c and Method S1 in the supporting information) [*Riley et al.*, 2011; *Ringeval et al.*, 2010; *Wania et al.*, 2010].

Table 1. Main Configuration of Three Model Experiments

		Data Description			Soil Forcing		
Experiment	Purpose	Soils	Period	Treatments	Temperature	Soil Moisture	Ensemble Design
Microcosm experiment [*Lau et al.*, 2015]	Parameterized high-affinity methanotrophs	Axel Heiberg Island, Canada	31 days	Six different temperature and soil moisture treatments	Prescribed from observations	Prescribed from observations	20 simulations parameterized with a random draw from the joint posterior probability density function derived from Markov chain Monte Carlo (MCMC) for methanotrophs
Core-thawing experiment [*Stackhouse et al.*, 2015]	Test methane fluxes at laboratory scales	Axel Heiberg Island, Canada	16 weeks	Control and moistened treatments	Prescribed from observations	Simulated using evaporation, precipitation, and redistribution	20 simulations parameterized with (1) same methanotroph parameters as microcosm experiment; and (2) methanogen parameters sampled from literature values
Field measurement [*Emmerton et al.*, 2014; *Jørgensen et al.*, 2015; *D'Imperio*, 2016]	Test methane fluxes at field scales	Canadian High arctic, Northeast and West Greenland	Jun–Sep	In situ observations at three dry tundra sites and one moist tundra site	Prescribed from observations (top 5 cm) and simulated using thermal conduction (bottom 95 cm)	Prescribed (top 5 cm) and simulated using redistribution (bottom 95 cm)	20 simulations initialized with same methanogen and methanotroph parameters as core-thawing experiment

2.2. Data Sets

Our models were parameterized and tested against measurements from microcosm and core-thawing experiments and field measurements [*Emmerton et al.*, 2014; *Jørgensen et al.*, 2015; *Lau et al.*, 2015; *Stackhouse et al.*, 2015; *D'Imperio*, 2016] (Table 1, Method S2, and Figure S1). All sites had SOC lower than 5%.

In a microcosm experiment, three replicates of 8–10 g of turbic cryosols from the Canadian High Arctic were incubated at different temperatures (4 and 10°C) and volumetric soil moistures (33, 66, and 100%) for 31 days [*Lau et al.*, 2015]. Headspace methane concentrations were monitored throughout the experiment to determine methane oxidation rates. These experiments were used to parameterize our model of high-affinity methanotrophy.

In a core-thawing experiment [*Stackhouse et al.*, 2015], a 16 week thaw was carried out mimicking in situ conditions using turbic cryosol cores of 1 m length and 7.5 cm diameter from the Canadian High Arctic. The cores were frozen at −4°C during transfer and storage. The cores thawed from the top down, finally reaching a uniform temperature of +4.5°C. Four cores received 40 mL of artificial rainwater each week (hereafter, "moistened" cores), whereas eight other cores did not receive any water (hereafter, "control" cores). The headspace of each core was flushed with a gas mixture at the start of each week for 16 weeks. For the first 14 weeks, the gas mixture was methane free and consisted of 79.0% N_2 and 20.5% O_2. For weeks 15 and 16, the gas mixture included 2 ppmv of methane.

We also used methane fluxes measured at four field sites: sparsely vegetated dwarf shrub on Ellesmere Island in the Canadian High Arctic instrumented during July 2011 [*Emmerton et al.*, 2014], dry and moist dwarf-shrub tundra sites in Northeast Greenland instrumented during July–September 2012 [*Jørgensen et al.*, 2015], and dry dwarf-shrub tundra in West Greenland instrumented during June–August 2013 [*D'Imperio*, 2016]. All sites had a mean air temperature of ~10°C during the study period. The dry tundra sites had a mean soil moisture of 15% (0–5 cm depth), and the moist tundra site had a mean soil moisture of 40%. The core-thawing experiments and the field measurements were used to evaluate our model at laboratory and field scales, respectively.

2.3. Model Experiments

We used the microcosm experiments to parameterize methanotrophy in our XHAM and HAM models. Simulations were forced with the observed temperature and soil water content data, and the simulated methane fluxes were compared to observations. Markov chain Monte Carlo was used to obtain the joint

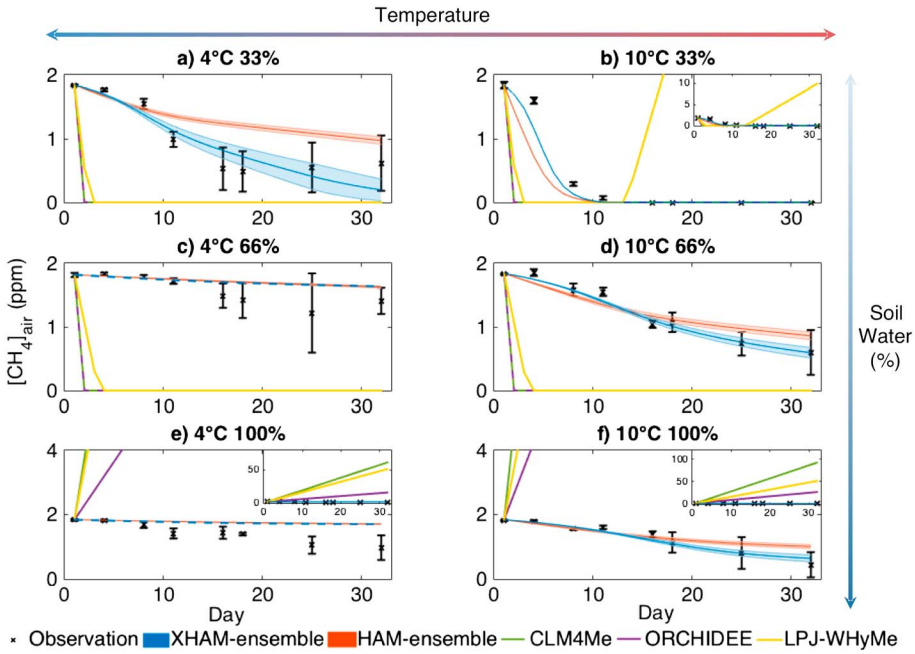

Figure 2. Model intercomparison of air methane concentration from microcosm experiments, XHAM and HAM ensembles, and three conventional models. Observational error bars represent 1 SD from three replicates and shaded intervals represent 1 SD from 20 ensemble members. Panel (a): temperature (T) of 4C, soil moisture as a percent of saturation (SM) of 33%. Panel (b): T=10C, SM=33%. Panel (c): T=4C, SM=66%. Panel (d): T=10C, SM=66%. Panel (e): T=4C, SM=100%. Panel (f): T=10C, SM=100%. In panels (c) and (e), then XHAM and HAM ensembles are very similar.

probability distribution of four parameters related to the soil temperature and moisture sensitivities of high-affinity methanotrophy (Method S3). We sampled the resulting probability distribution 20 times and used these samples to define 20 different model ensemble members (Method S3 and Tables S5 and S6). Full listings of parameter values are given in Tables S1 and S2. Simulations under microcosm conditions were repeated for each ensemble member.

We simulated the core-thawing experiments with each ensemble member. In each simulation, initial conditions for methane, acetate concentrations, and temporal changes of soil temperature were based on observed values [*Stackhouse et al.*, 2015]. Because soil moisture was not measured, we simulated it using a simple model (Method S2.2).

We also carried out ensemble simulations of the four sites in the Canadian High Arctic and Greenland. Time series of soil temperature and moisture of the top 5 cm during the study period were prescribed from observations. Because soil temperature and moisture dynamics below 5 cm depth were not measured, we simulated them using thermal conduction and redistribution models (Method S2.3).

3. Results

3.1. Microcosm Experiment

The simulated methane fluxes from XHAM and HAM are generally consistent with observational data (mean R^2 values of 0.86 and 0.72, respectively) (Figure 2). This result was expected because XHAM and HAM were parameterized using these data. The largest model biases correspond to water-saturated conditions (Figure 2e). Overall, the conventional models (CLM4Me, ORCHIDEE, and LPJ-WhyMe) show larger biases than XHAM or HAM. Under unsaturated conditions, they mostly simulate complete consumption of methane within 2 days, except 10°C 33% conditions for LPJ-WhyMe (Figures 2a–2d); under saturated conditions, all conventional models simulate strong net methane emission (Figures 2e and 2f).

To investigate the effect of microbial biomass changes, we compared the daily methane oxidation rate simulated by HAM and XHAM to the observed rates (Figure S2). Both observations and XHAM show bell-shaped

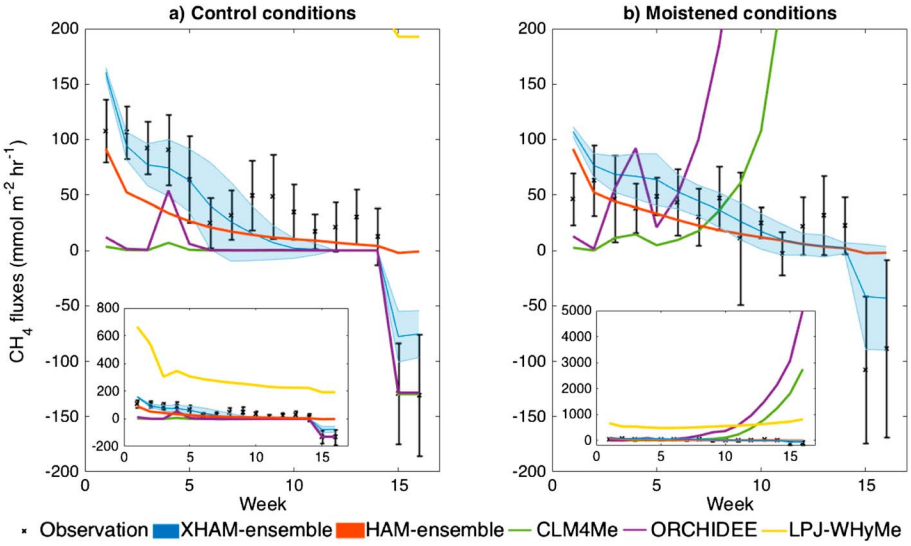

Figure 3. Methane fluxes from the core-thawing experiments and model simulations. Shown are (a) control conditions and (b) moistened conditions. Error bars and shading both represent 1 SD.

curves. In XHAM, the initial increase corresponds to a transient increase in active methanotrophic biomass by 4 (10°C 66, 100%, and 4°C, 33% conditions) to 10 times (10°C, 33% conditions), and the decline corresponds to the gradual reduction in methane concentration. In contrast, HAM simulates its maximum daily methane oxidation at the beginning of the experiment and oxidation monotonically declines as methane concentration decreases. Residual error in the XHAM simulations may be due to errors in model parameters that were taken from the literature, including those relevant to microbial biomass accumulation and turnover (equation (S3-2)). Furthermore, the model does not account for the possibility of methanotrophs consuming substrates other than methane under low-methane conditions.

3.2. Soil Core-Thawing Experiment

XHAM simulations are broadly consistent (mean R^2 of 0.73) with the observed methane fluxes from soil core-thawing experiments (Figure 3). Emissions are initially large but decrease throughout the first 6 weeks of the experiment. Supplementary simulations with microbial activity deactivated show a similar signal in weeks 1–6 (Figure S3), indicating that the week 1–6 response corresponds to the release of methane gas trapped during the last freeze-in and wintertime periods [*Stackhouse et al.*, 2015]. Compared to the control cores, less methane is released from the moistened cores during the initial 6 weeks (Figure 3b), which the model attributes to slower diffusion of methane through water-filled pore space. Additionally, the XHAM simulations capture the rapid methane uptake that occurs during weeks 15 through 16, when 2 ppmv of methane was introduced to the headspace.

HAM simulates methane emission from the core in weeks 1–6, but simulates negligible methane oxidation in weeks 15–16 (Figure 3). The difference between XHAM and HAM simulations occurs because only XHAM includes a buildup of active methanotroph biomass. These biomass increases coincide with increases in temperature and rates of methanogenesis. We found that the differences between the XHAM and HAM simulations were due to the dynamics of active biomass changes in XHAM rather than differences in model parameters (Figure S4).

CLM4Me and ORCHIDEE simulate methane consumption under control conditions (Figure 3a). In these models, methane production is restricted if the soil is not fully saturated. For saturated soils (Figure 3b), CLM4Me and ORCHIDEE simulate large rates of methane emission. LPJ-WHyMe simulates methane emission for both control and moistened conditions because its soil moisture sensitivity function is more permitting of methanogenesis under subsaturated conditions (Table S3).

3.3. Field Measurements

XHAM captures the large methane uptake from the four field sites throughout the summer ($-6.52 \pm 2.61\ \mu mol\ m^{-2}\ h^{-1}$, 1 SD) (Figure 4). The HAM model is nearly neutral ($-0.21 \pm 0.39\ \mu mol\ m^{-2}\ h^{-1}$, 1 SD).

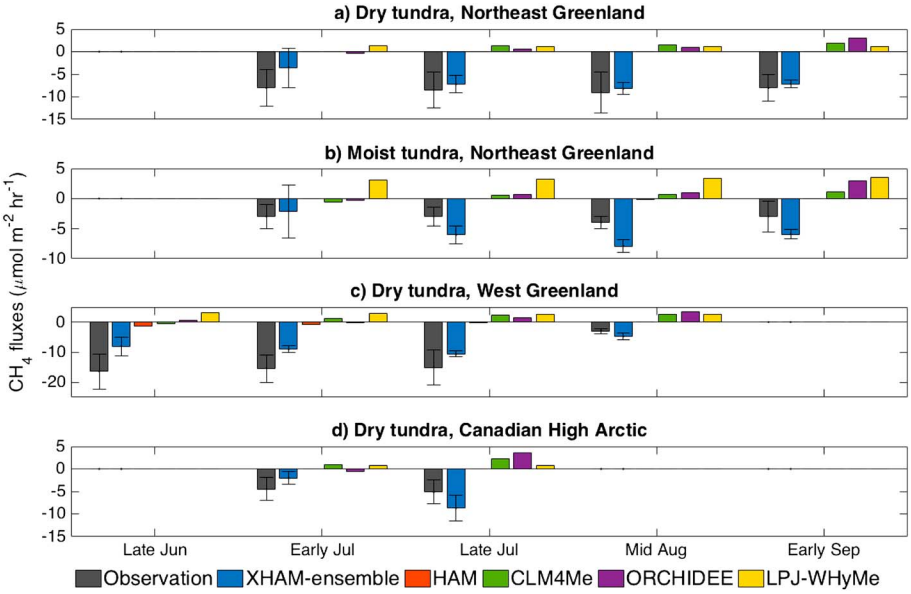

Figure 4. Comparison of simulated and observed methane fluxes from (a–d) four field sites.

The three conventional models typically simulate emission of methane from the soil or are nearly neutral ($+1.49 \pm 1.27$ μmol m^{-2} h^{-1}, 1 SD). These results are of same magnitude as those from methane model intercomparison studies [*Tan et al.*, 2015; *Melton et al.*, 2013; *Wania et al.*, 2013]. LPJ-WhyMe simulates the highest methane emission rate in moist tundra because of its soil moisture sensitivity function (Table S3). In contrast, CLM4Me simulates less emission from moist tundra than from dry tundra because its optimal methane oxidation occurs at 60–80% of water saturation (Figure S5). The methane fluxes from ORCHIDEE range from small negative to large positive fluxes during the growing season because of its high temperature sensitivity of methane production (Q_{10} of 6) relative to methane oxidation (Q_{10} of 2) (Table S3).

4. Discussion

Our results emphasize the importance of simulating high-affinity methanotrophy and active microbial biomass changes. For different experimental scales, site locations, and soil moisture conditions, the XHAM model accurately simulates methane uptake from arctic mineral soils. Models that do not include microbial biomass dynamics or do not parameterize high-affinity methanotrophy exhibit significant biases. Incorporation of high-affinity methanotrophy into mechanistic methane models may improve the comparison between models and atmospheric inversions [*Aronson et al.*, 2013; *Kirschke et al.*, 2013].

Our parameterization of high-affinity methanotrophs reflects their unique physiology. We infer a temperature sensitivity for high-affinity methanotrophy (117 kJ mol^{-1}, Table S2) that is higher than the temperature sensitivity of methanogenesis (106 kJ mol^{-1}) [*Allen et al.*, 2005; *Yvon-Durocher et al.*, 2014] and 2–3 times higher than the temperature sensitivity of low-affinity methanotrophy [*Jang et al.*, 2006]. In contrast, current methane models parameterize the temperature sensitivity of methanotrophy to be 1–3 times smaller than the temperature sensitivity of methanogenesis (Figure S5). Moreover, the microcosm and core-thawing experiments reveal that methane oxidation was possible under saturated conditions; however, some of the conventional mechanistic models require aerobic conditions for methanotrophs to oxidize methane.

Taken together, these results have implications for our understanding and modeling of arctic methane fluxes (Figure 5). Previous studies predicted a positive feedback between temperature and methane emission, whereby increased temperature triggers permafrost thaw, which increases soil moisture, further increasing methane emission by methanogenesis (Figure 5, circles 1–2) [*Hinzman et al.*, 2013]. However, this framework does not account for the physiology of high-affinity methanotrophs. Because high-affinity methanotrophs may respond more strongly to temperature and less strongly to soil moisture than low-affinity methanotrophs (Figure 5, circles 3–4), this feedback loop may be partially suppressed.

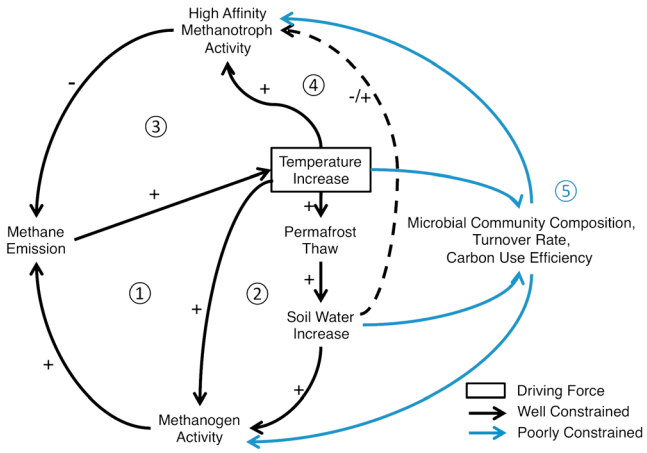

Figure 5. Future arctic methane feedbacks. The arctic methane feedback is initiated by temperature increases and is a combination of moderately constrained (black lines) and poorly constrained (blue lines) processes. Plus and minus signs indicate positive and negative feedbacks, respectively. The dashed line indicates combined positive and negative feedbacks depending on the range of soil water increases. The circled numbers are described in the text.

Accounting for seasonal biomass changes improved our simulations of core-thawing experiments and field observations. Such seasonal biomass changes are likely important for annual methane budgets. For example, increases in the thaw season length will likely have a nonlinear effect on microbial productivity [*Roy Chowdhury et al*., 2015]. Moreover, explicit modeling of microbial dynamics (Figure 5, circle 5) will facilitate future model developments that include effects of microbial adaptation [*Graham et al*., 2012].

Circumpolar application of our XHAM model will require additional work. First, the current model was parameterized using data from a limited set of microcosm experiments. Additional data, corresponding to a wider range of soil temperatures and moisture contents, would be helpful to generalize the model. Second, SOC varies throughout the Arctic and exerts a first-order control on arctic methane fluxes; a future priority should be to evaluate models at sites having a broader range of SOC. Such work will better allow us to test the interplay between high-affinity methanotrophs, low-affinity methanotrophs, and different classes of methanogens. Currently, our model is perhaps best suited for dry, mineral cryosols, where high-affinity methanotrophy has been shown to be important [*Lau et al*., 2015]. The role of methane-oxidizing archaea should also be explored [*Hu et al*., 2014; *Segarra et al*., 2015; *Shelley et al*., 2015]. Lastly, experiments should be done to better constrain microbial dynamics in models to facilitate better prediction and understanding of arctic methane budgets.

Acknowledgments
We acknowledge support from the Danish National Research Foundation (CENPERM DNRF100) and Natural Sciences and Engineering Research Council of Canada (NSERC). We thank William Riley, Shuhei Ono, Jaya Khanna, and two anonymous reviewers for helpful comments. The data and model code are available upon request to the authors.

References

Allen, A., J. Gillooly, and J. Brown (2005), Linking the global carbon cycle to individual metabolism, *Funct. Ecol.*, *19*(2), 202–213.
Aronson, E. L., S. D. Allison, and B. R. Helliker (2013), Environmental impacts on the diversity of methane-cycling microbes and their resultant function, *Frontiers Microbiol.*, *4*.
Brummell, M. E., R. E. Farrell, S. P. Hardy, and S. D. Siciliano (2014), Greenhouse gas production and consumption in High Arctic deserts, *Soil Biol. Biochem.*, *68*, 158–165.
Christiansen, J. R., A. J. B. Romero, N. O. Jørgensen, M. A. Glaring, C. J. Jørgensen, L. K. Berg, and B. Elberling (2015), Methane fluxes and the functional groups of methanotrophs and methanogens in a young Arctic landscape on Disko Island, West Greenland, *Biogeochemistry*, *122*(1), 15–33.
Conrad, R. (2009), The global methane cycle: Recent advances in understanding the microbial processes involved, *Environ. Microbiol. Rep.*, *1*(5), 285–292.
D'Imperio, L. (2016), Methane and root dynamics in Arctic soils: responses to experimental summer warming and winter snow accumulation, PhD thesis, Univ. of Copenhagen, Copenhagen.
Emmerton, C. A., V. St Louis, I. Lehnherr, E. R. Humphreys, E. Rydz, and H. R. Kosolofski (2014), The net exchange of methane with high Arctic landscapes during the summer growing season, *Biogeosciences*, *11*(12), 3095–3106.
Graham, D. E., M. D. Wallenstein, T. A. Vishnivetskaya, M. P. Waldrop, T. J. Phelps, S. M. Pfiffner, T. C. Onstott, L. G. Whyte, E. M. Rivkina, and D. A. Gilichinsky (2012), Microbes in thawing permafrost: The unknown variable in the climate change equation, *ISME J.*, *6*(4), 709–712.
Hinzman, L. D., C. J. Deal, A. D. McGuire, S. H. Mernild, I. V. Polyakov, and J. E. Walsh (2013), Trajectory of the Arctic as an integrated system, *Ecol. Appl.*, *23*(8), 1837–1868.
Hu, B.-L., L.-D. Shen, X. Lian, Q. Zhu, S. Liu, Q. Huang, Z.-F. He, S. Geng, D.-Q. Cheng, and L.-P. Lou (2014), Evidence for nitrite-dependent anaerobic methane oxidation as a previously overlooked microbial methane sink in wetlands, *Proc. Natl. Acad. Sci. U.S.A.*, *111*(12), 4495–4500.
Hugelius, G., J. Strauss, S. Zubrzycki, J. W. Harden, E. Schuur, C.-L. Ping, L. Schirrmeister, G. Grosse, G. J. Michaelson, and C. D. Koven (2014), Estimated stocks of circumpolar permafrost carbon with quantified uncertainty ranges and identified data gaps, *Biogeosciences*, *11*(23), 6573–6593.
Jang, I., S. Lee, J.-H. Hong, and H. Kang (2006), Methane oxidation rates in forest soils and their controlling variables: A review and a case study in Korea, *Ecol. Res.*, *21*(6), 849–854.
Jørgensen, C. J., K. M. L. Johansen, A. Westergaard-Nielsen, and B. Elberling (2015), Net regional methane sink in High Arctic soils of northeast Greenland, *Nat. Geosci.*, *8*(1), 20–23.
King, G. M. (1994), Associations of methanotrophs with the roots and rhizomes of aquatic vegetation, *Appl. Environ. Microbiol.*, *60*(9), 3220–3227.

Kirschke, S., P. Bousquet, P. Ciais, M. Saunois, J. G. Canadell, E. J. Dlugokencky, P. Bergamaschi, D. Bergmann, D. R. Blake, and L. Bruhwiler (2013), Three decades of global methane sources and sinks, *Nat. Geosci.*, *6*(10), 813–823.

Koven, C. D., W. J. Riley, and A. Stern (2013), Analysis of permafrost thermal dynamics and response to climate change in the CMIP5 Earth System Models, *J. Clim.*, *26*(6), 1877–1900.

Lau, M., et al. (2015), An active atmospheric methane sink in high Arctic mineral cryosols, *ISME J.*, *9*, 1880–1891.

Le Mer, J., and P. Roger (2001), Production, oxidation, emission and consumption of methane by soils: A review, *Eur. J. Soil Biol.*, *37*(1), 25–50.

Martineau, C., Y. Pan, L. Bodrossy, E. Yergeau, L. G. Whyte, and C. W. Greer (2014), Atmospheric methane oxidizers are present and active in Canadian high Arctic soils, *FEMS Microbiol. Ecol.*, *89*(2), 257–269.

McGuire, A. D., L. G. Anderson, T. R. Christensen, S. Dallimore, L. Guo, D. J. Hayes, M. Heimann, T. D. Lorenson, R. W. Macdonald, and N. Roulet (2009), Sensitivity of the carbon cycle in the Arctic to climate change, *Ecol. Monogr.*, *79*(4), 523–555.

Melton, J., R. Wania, E. Hodson, B. Poulter, B. Ringeval, R. Spahni, T. Bohn, C. Avis, D. Beerling, and G. Chen (2013), Present state of global wetland extent and wetland methane modelling: Conclusions from a model intercomparison project (WETCHIMP), *Biogeosciences*, *10*, 753–788.

Riley, W., Z. Subin, D. Lawrence, S. Swenson, M. Torn, L. Meng, N. Mahowald, and P. Hess (2011), Barriers to predicting changes in global terrestrial methane fluxes: analyses using CLM4Me, a methane biogeochemistry model integrated in CESM, *Biogeosciences*, *8*(7), 1925–1953.

Ringeval, B., N. de Noblet-Ducoudré, P. Ciais, P. Bousquet, C. Prigent, F. Papa, and W. B. Rossow (2010), An attempt to quantify the impact of changes in wetland extent on methane emissions on the seasonal and interannual time scales, *Global Biogeochem. Cycles*, *24*, GB2003, doi:10.1029/2008GB003354.

Roy Chowdhury, T., E. M. Herndon, T. J. Phelps, D. A. Elias, B. Gu, L. Liang, S. D. Wullschleger, and D. E. Graham (2015), Stoichiometry and temperature sensitivity of methanogenesis and CO_2 production from saturated polygonal tundra in Barrow, Alaska, *Global Change Biol.*, *21*(2), 722–737.

Schaefer, K., T. Zhang, L. Bruhwiler, and A. P. Barrett (2011), Amount and timing of permafrost carbon release in response to climate warming, *Tellus B*, *63*(2), 165–180.

Schuur, E., B. Abbott, W. Bowden, V. Brovkin, P. Camill, J. Canadell, J. Chanton, F. Chapin III, T. Christensen, and P. Ciais (2013), Expert assessment of vulnerability of permafrost carbon to climate change, *Clim. Change*, *119*(2), 359–374.

Segarra, K., F. Schubotz, V. Samarkin, M. Yoshinaga, K. Hinrichs, and S. Joye (2015), High rates of anaerobic methane oxidation in freshwater wetlands reduce potential atmospheric methane emissions, *Nat. Commun.*, *6*.

Shelley, F., F. Abdullahi, J. Grey, and M. Trimmer (2015), Microbial methane cycling in the bed of a chalk river: Oxidation has the potential to match methanogenesis enhanced by warming, *Freshwater Biol.*, *60*(1), 150–160.

Shukla, P. N., K. Pandey, and V. K. Mishra (2013), Environmental determinants of soil methane oxidation and methanotrophs, *Critical Rev. Environ. Sci. Technol.*, *43*(18), 1945–2011.

Stackhouse, B. T., T. A. Vishnivetskaya, A. Layton, A. Chauhan, S. Pfiffner, N. C. Mykytczuk, R. Sanders, L. G. Whyte, L. Hedin, and N. Saad (2015), Effects of simulated spring thaw of permafrost from mineral cryosol on CO_2 emissions and atmospheric CH_4 uptake, *J. Geophys. Res. Biogeosci.*, *120*, 1764–1784, doi:10.1002/2015JG003004.

Tan, Z., Q. Zhuang, D. Henze, C. Frankenberg, E. Dlugokencky, C. Sweeney, and A. Turner (2015), Mapping pan-Arctic methane emissions at high spatial resolution using an adjoint atmospheric transport and inversion method and process-based wetland and lake biogeochemical models, *Atmos. Chem. Phys. Discuss.*, *15*(22), 32,469–32,518.

Wania, R., I. Ross, and I. Prentice (2010), Implementation and evaluation of a new methane model within a dynamic global vegetation model: LPJ-WHyMe v1. 3.1, *Geosci. Model Dev.*, *3*(2), 565–584.

Wania, R., J. Melton, E. Hodson, B. Poulter, B. Ringeval, R. Spahni, T. Bohn, C. Avis, G. Chen, and A. Eliseev (2013), Present state of global wetland extent and wetland methane modelling: Methodology of a model inter-comparison project (WETCHIMP), *Geosci. Model Dev.*, *6*(3), 617–641.

Xu, X., D. A. Elias, D. E. Graham, T. J. Phelps, S. L. Carroll, S. D. Wullschleger, and P. E. Thornton (2015), A microbial functional group-based module for simulating methane production and consumption: Application to an incubated permafrost soil, *J. Geophys. Res. Biogeosci.*, *120*, 1315–1333, doi:10.1002/2015JG002935.

Yvon-Durocher, G., A. P. Allen, D. Bastviken, R. Conrad, C. Gudasz, A. St-Pierre, N. Thanh-Duc, and P. A. Del Giorgio (2014), Methane fluxes show consistent temperature dependence across microbial to ecosystem scales, *Nature*, *507*(7493), 488–491.

Zhu, R., Q. Chen, W. Ding, and H. Xu (2012), Impact of seabird activity on nitrous oxide and methane fluxes from High Arctic tundra in Svalbard, Norway, *J. Geophys. Res.*, *117*, G04015, doi:10.1029/2012JG002130.

Zhuang, Q., M. Chen, K. Xu, J. Tang, E. Saikawa, Y. Lu, J. M. Melillo, R. G. Prinn, and A. D. McGuire (2013), Response of global soil consumption of atmospheric methane to changes in atmospheric climate and nitrogen deposition, *Global Biogeochem. Cycles*, *27*, 650–663, doi:10.1002/gbc.20057.